

# Microstructure and Properties of Non-Quenched/Tempered Seamless Tubes Made of Medium Carbon V-microalloyed Steel

LIU Guo-quan<sup>1</sup>, LIU Sheng-xin<sup>1</sup>, ZHONG Yun-long<sup>1</sup>, ZHANG Yong-gang<sup>2</sup>, FENG Shun<sup>2</sup>

(1. School of Materials Science and Engineering, University of Science and Technology Beijing, Beijing 100083, China;

2. Wuxi Seamless Special Steel Tube Co. Ltd, Wuxi 214026, China)

**Abstract:** Hot rolling non-quenched and tempered (NQT) tube manufacturing process consists of a series of sub-processes such as billet-heating, piercing, tube-rolling, intermediate cooling, reheating, stretch-reduction-diameter, and final cooling. Both industrial experiments of production of seamless tubes using a medium carbon vanadium microalloyed steel and corresponding laboratory compression simulation with a Gleeble thermal/dynamic simulator were carried out. First, it is found that the most effective microstructure refinement did not occur in austenite state, but mainly in austenite decomposition following the stretch-reduction-diameter process, and the intragranular ferrite formation should be very useful for effective refinement of the whole microstructure. Second, more than half of precipitates in final tubes were formed in stretch-reduction-diameter and final cooling processes. Third, the results show that proper selection of intermediate cooling stop temperature  $T_{stop}$  is of vital importance in order to achieve desired microstructure and optimized combination of strength and toughness, though no austenite  $\leftrightarrow$  ferrite transformation occur during the intermediate cooling and reheating. Compared with that using  $T_{stop}=850^{\circ}\text{C}$  which may lead to harmful bainite and bainite-like constituents, the NQT tube manufacture process using  $T_{stop}=600^{\circ}\text{C}$  results to finer microstructure and much larger amount of intra-granular ferrite, much larger fraction and finer particle size of precipitates in final tube products.

**Key words:** seamless tubes; vanadium microalloyed steels; hot rolling; precipitation; intra-granular ferrite

## 1 Introduction

The petroleum seamless casing and tubing are almost all manufactured with heat treatments such as quenching and high temperature tempering of the tubes. In order to avoid such heat treatments for energy and cost saving while keeping desirable properties, both development of new vanadium-containing non-quenched and tempered (NQT) steels and optimization of corresponding tube manufacturing process are of great significance. This is true especially for China, a country rich in vanadium resources.

The hot rolling NQT seamless tube manufacturing process consists of a series of sub-processes such as billet heating (soaking), piercing, tube rolling, intermediate controlled cooling, reheating, stretch-reduction-diameter, and final cooling. Thus, in such a process the situation is more complicated than the common hot rolling or forging cases. Most previous studies on V-microalloyed steels paid more attentions to low-carbon ones, while recent studies

have further shown that the phase transformation characteristics and precipitation strengthening in V-microalloyed steels are different significantly for low- and medium-carbon steels [1-4]. Due to such complexities, the understanding of microstructural mechanisms underlying the NQT seamless tube manufacturing process, especially in the practical industrial production, is quite limited.

The aim of this paper is mainly to achieve a better understanding of the microstructure evolution, including grain size variation as well as microalloying precipitation, and their effect on mechanical properties in medium carbon V-microalloyed steels during industrial NQT seamless tube manufacturing process, largely based on our previous work carried out at the University of Science and Technology Beijing and Wuxi Seamless Steel Tube Co. Ltd. during 2001-2004 [1,3-8].

## 2 Materials and Methods

The steel studied was a medium carbon V-Ti-N

Foundation item: Item supported by National Natural Science Foundation of China (No.50271009, 50334010), and by the VANITEC via the CSM.

Biography: LIU Guo-quan (1952), Male, Ph.D.:Professor, E-mail: [g.liu@ustb.edu.cn](mailto:g.liu@ustb.edu.cn)



microalloyed steel designed as a Chinese grade 33Mn2V, containing 0.30-0.40 C, 0.29-0.40 Si, 1.40-1.69 Mn, Ti <0.02, V <0.12, N <0.014, all in wt% with Fe as balance. The material was received in the form of 100 mm diameter solid billets produced by continuous casting and continuous rolling technology, while the final tube products were designed as N80-grade  $\phi 73 \times 5.51$  mm NQT seamless casing and tubing for petroleum oil wells.

The tube manufacture layout with  $\phi 100$  mm ASSEL rollers used for industrial experiments is shown in Fig. 1(a). Laboratory compression simulation of such an industrial process was carried out with a Gleeble 1500 thermal/dynamic simulator as shown in Fig. 1(b). For the purpose of comparison, two different intermediate cooling stop temperatures,  $T_{\text{stop}}=850^\circ\text{C}$  and  $600^\circ\text{C}$ , were used in the experiments.

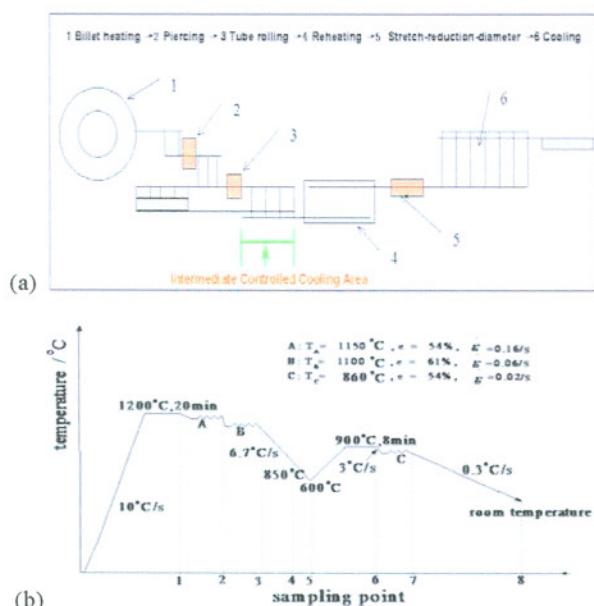


Fig. 1 Industrial layout (a) and laboratory simulation schedule (b) for manufacturing NQT seamless tubes

Metallographic samples and optical examinations were prepared and carried out using standard methods. Grain size of prior austenite or ferrite and volume fraction of ferrite were measured from optical micrographs employing linear intercept method and point count method [9], respectively. The results are reported with a relative error of less than 5%. The weight fraction and particle size distribution data of precipitates were based on chemical extracted precipitates in given steel samples. The

precipitation-time-temperature (PTT) diagram for vanadium carbonitrides V(C,N) in deformed austenite was experimentally determined using a modified stress-relaxation technique [4], with a Gleeble 2000 thermal/dynamic simulator. The samples were heated at  $1200^\circ\text{C}$  for 600s, then cooled down to the deformation/precipitation temperature with a rate of  $30\text{ K}\cdot\text{s}^{-1}$ . The thermo-chemical calculation for precipitation in the steel was carried out in the way as mentioned in [4].

The CCT diagram of the steel was determined using both a Formaster digital automatic dilatometer and a Gleeble 1500 thermal/dynamic simulator [1].

### 3 Results and Discussion

#### 3.1 Austenite decomposition

Fig. 2 shows the CCT diagram experimentally determined by holding the samples at  $1200^\circ\text{C}$  for 20min followed by double hot deformation at  $1150^\circ\text{C}$  and  $1100^\circ\text{C}$ , with the PTT diagram of V(C,N) superimposing on the same figure. It clearly shows that the austenite in this steel does not undergo decomposition during intermediate cooling down to as low as  $600^\circ\text{C}$  after tube rolling, with a cooling rate faster than  $4\text{ K}\cdot\text{s}^{-1}$ .

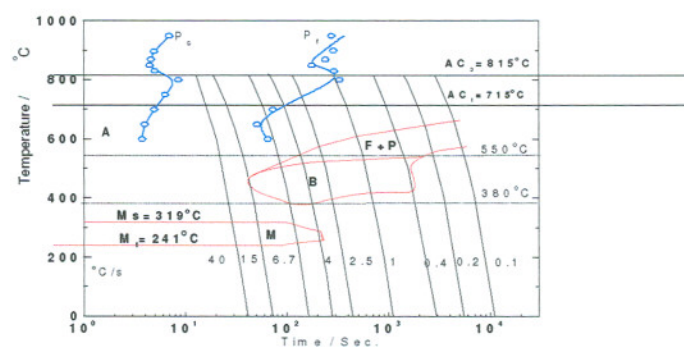


Fig. 2 PTT curve of V-bearing precipitates superimposed upon the CCT diagram of the experimental steel

#### 3.2 Grain size and microstructure refinement

It has been known from our previous study [5] that the experimental steel has good anti-coarsening ability at elevated temperatures. The actual average grain size in soaked billets is usually about  $21\mu\text{m}$  or corresponding to ASTM grain size grade  $G \approx 8$ . It is easy to be understood since trace Ti was added in the steel as austenite grain growth prohibitor.

Many industrial experts previously thought that the



grains would be continuously refined in the tube manufacture process shown in Fig.1. However, the austenite grain size data in Fig.3 show that it is not true. The corresponding microstructures in both simulated and industrial samples are shown in Fig.4. It is seen from all the three plots in Fig.3 that the average austenite grain size reached in reheated stage is  $G=6$  or  $d_\gamma \approx 41\mu\text{m}$ . It seems that the austenite grains are coarser in the case of  $T_{\text{stop}}=600^\circ\text{C}$  compared with that  $T_{\text{stop}}=850^\circ\text{C}$ . Even in the case after the deformation in stretch-reduction-diameter stage, the austenite grain size is not finer than that at piercing starting point.

Fig.5 shows the microstructures in the samples at sampling point 8, i.e., the final products. It is easy to see that the schedule with  $T_{\text{stop}}=600^\circ\text{C}$  led to much finer microstructures and a large amount of intra-granular ferrite either in industrial experiment or laboratory simulation, while that schedule with  $T_{\text{stop}}=850^\circ\text{C}$  led to grain boundary networked and less ferrite, even to harmful bainite. In Fig.5(c), intra-granular ferrite was found almost everywhere except for few areas inside prior austenite grains.

From Fig.3 to Fig.5, it is concluded that *the most effective microstructure refinement did not occur in austenite state, but mainly in austenite decomposition process following the stretch-reduction-diameter, and the intra-granular ferrite formation should be very useful for effective refinement of the whole microstructure.*

**Table 1** summarizes quantitative results on microstructure examination and mechanical tests of industrial hot-rolled NQT seamless tube samples. It further shows that the schedule with  $T_{\text{stop}}=600^\circ\text{C}$  led

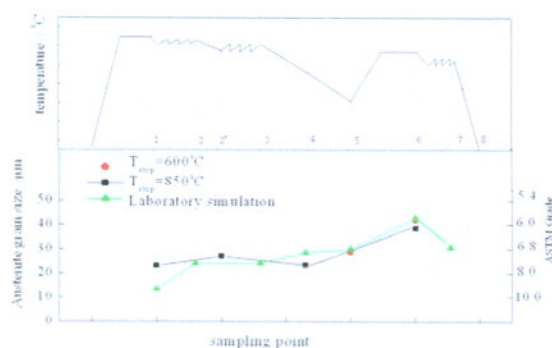


**Fig. 3** Variation of austenite grain size in the tube manufacture process shown in Fig.1(b)

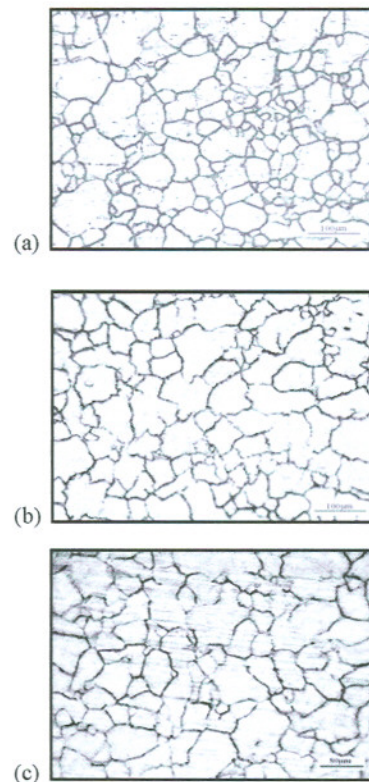


**Fig. 4** Austenite microstructures in samples at sampling point 6 in Fig.1(b) or Fig.3. (a) Simulated,  $T_{\text{stop}} = 850^\circ\text{C}$ ; (b) Simulated,  $600^\circ\text{C}$ ; (c) Industrial,  $600^\circ\text{C}$

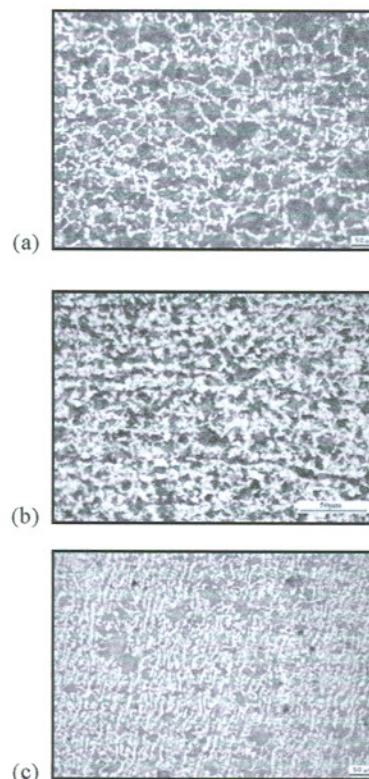


**Fig. 5** Microstructures in samples at sampling point 8 in Fig.1(b) or Fig.3. (a) Industrial,  $T_{\text{stop}} \approx 850^\circ\text{C}$ ; (b) Simulated,  $T_{\text{stop}} = 600^\circ\text{C}$ ; (c) Industrial,  $T_{\text{stop}} \approx 600^\circ\text{C}$

to much more ferrite with smaller grain size in industrial experiments than that with  $T_{\text{stop}}=850^{\circ}\text{C}$ .

**Table 1** Microstructures and properties of industrial seamless tube samples

| Samples   | Microstructure <sup>a</sup> | Ferrite                                       |                   |                                      |
|---|-----------------------------|---|-------------------|--------------------------------------|
|   |                             | Volume %                                      | Type <sup>b</sup> | $\alpha$ -grain size / $\mu\text{m}$ |
| A-1<br>( $T_{\text{stop}}=600^{\circ}\text{C}$ )        | F+P                         | 42.3  | NGB               | 5.2 $\pm$ 2.0                        |
| A-2<br>( $T_{\text{stop}}=850^{\circ}\text{C}$ )        | F+P+B+(B-like)              | 15.6  | GB                | 7.2 $\pm$ 3.2                        |
| B-1<br>( $T_{\text{stop}}\approx 600^{\circ}\text{C}$ ) | F+P                         | 42.1  | NGB               | 6.0 $\pm$ 3.5                        |
| B-2<br>( $T_{\text{stop}}\approx 850^{\circ}\text{C}$ ) | F+P+ (B-like)               | 22.1  | GB                | 10.0 $\pm$ 6.6                       |
| (continued)   |                             |   |                   |                                      |
| Bainite and bainite-like constituents                   |                             | UTS   | YS                | Elongation                           |
|   |                             | MPa   | MPa               | %                                    |
|   |                             | V-notch impact energy at 0 $^{\circ}\text{C}$ |                   |                                      |
|   |                             | J   |                   |                                      |
| Volume %  |                             |   |                   |                                      |
| 0   | 765                         | 585   | 19                | 36,36,36                             |
| 43  | 915                         | 685   | 16                | 13,18,16                             |
| 0   | 840                         | 585   | 20                | 42                                   |
| 5.5   | 830                         | 565   | 17                | 11                                   |

Notes: a: F=ferrite, P=pearlite, B=bainite; b: GB=grain boundary networked, NGB=non-GB networked.

### 3.3 Characterization of Precipitates

The double C-curved isothermal precipitation-time-temperature (PTT) diagram in austenite was experimentally determined using stress relaxation method and superimposed onto the CCT diagram as shown in Fig.3. It is seen from the PTT diagram that the V(C,N) precipitation would occur in cooling process down to temperatures even lower than  $600^{\circ}\text{C}$  in the experimental steel. However, since the cooling rate before the isothermal precipitation used in PTT diagram determination was  $30\text{ K}\cdot\text{s}^{-1}$ , much higher than the rate of intermediate cooling used in industrial process, the driving force for the precipitation at lower

temperature range around  $600^{\circ}\text{C}$  would be much smaller than that in the case of PTT diagram determination.

The precipitates in stress relaxation samples were experimentally identified as mainly V(C,N) or (Ti,V)(C,N) particles, with the latter mostly being V(C,N) covered on TiN cores. It is also found that the lower the precipitation temperature is, the higher the mole fraction of carbon in V(C,N). This fact is further supported by the calculation results shown in Fig.6.

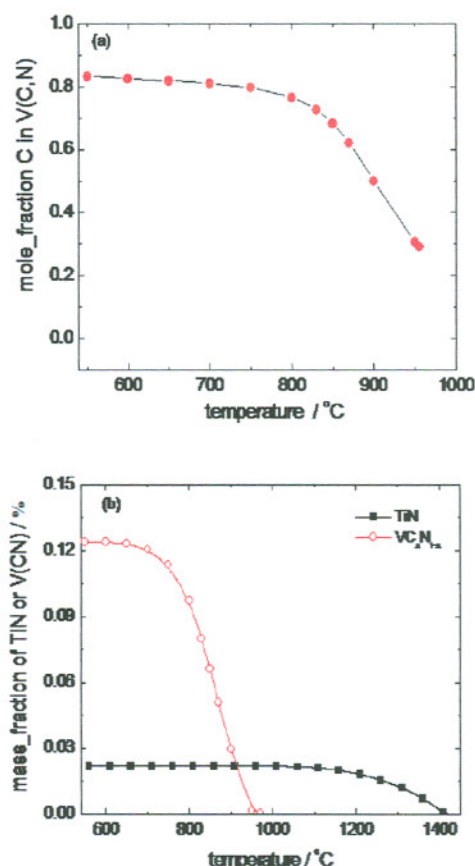


**Fig. 6** Thermo-chemical calculation results for a steel with 0.35C-1.56Mn-0.1V-0.011N-0.017Ti (wt.%), showing the C content in V(C,N) and the relative amounts of V(C,N) or TiN in austenite at different temperatures.

The experimental data of weight fraction and mean particle size of MN+M(C,N) precipitates in industrial samples are summarized in Table 2, where M stands for V and Ti. It is seen that more than half (65% for the case of  $T_{\text{stop}}=600^{\circ}\text{C}$ ) of precipitates in final tubes were formed in stretch-reduction-diameter and final cooling processes.



Fig.7 shows the histograms of MN+M(C,N) precipitate size distribution extracted from finished tubes resulted from the schedules with  $T_{\text{stop}}=600^{\circ}\text{C}$  and  $850^{\circ}\text{C}$ , and their corresponding TEM micrographs. Compared with that using  $T_{\text{stop}}=850^{\circ}\text{C}$  (Fig.7(b), (d) and Table 2), the NQT tube manufacture process using  $T_{\text{stop}}=600^{\circ}\text{C}$  resulted to much larger amount and finer particle size of precipitates (Fig.7(a), (c) and Table 2) in final tube products. What is more, the particle size distribution has a desired shape in the latter case.

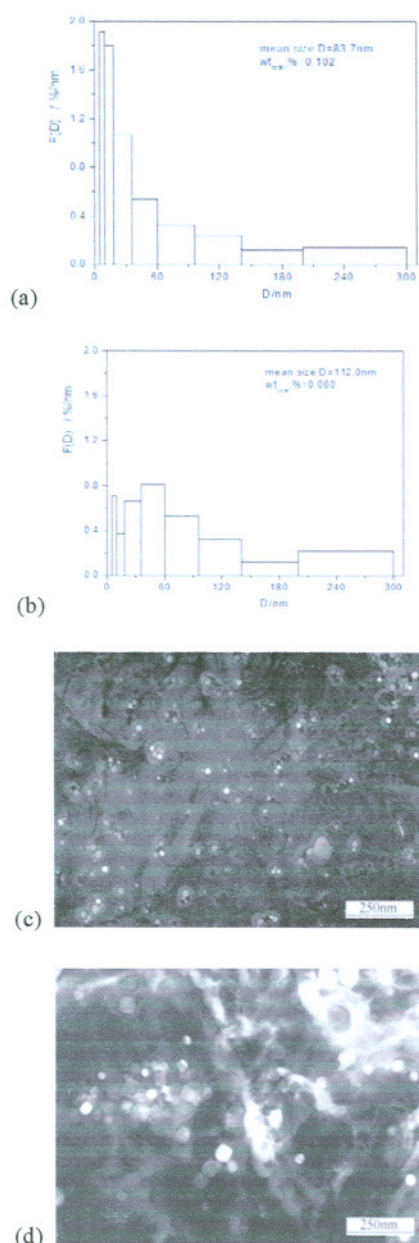


Fig. 7 Histograms of size distribution of MC+M(C,N) precipitates extracted from finished tubes resulted from reheating from  $600^{\circ}\text{C}$  (a) and  $850^{\circ}\text{C}$  (b); and corresponding TEM micrographs (c) and (d), respectively.

Table 2 Weight fraction and mean size of MN+M(C,N) precipitates in industrial experiment samples

| $T_{\text{stop}}$<br>/ $^{\circ}\text{C}$ | Cooled to $T_{\text{stop}}$<br>after tube rolling,<br>then quenched |                 | At the end of<br>reheating<br>at $900^{\circ}\text{C}$ , then<br>quenched |                 | Final tube<br>samples |                 |
|---|---|-----------------|---|-----------------|-----------------------|-----------------|
|   | Weight<br>fraction  | Mean<br>size    | Weight<br>fraction  | Mean<br>size    | Weight<br>fraction    | Mean<br>size    |
|   | / %   | / $\mu\text{m}$ | / %   | / $\mu\text{m}$ | / %                   | / $\mu\text{m}$ |
| 600                                       | 0.029   | 145.8           | 0.036   | 99.1            | 0.102                 | 83.7            |
| 850                                       | 0.029   | 145.0           | 0.028   | 97.9            | 0.060                 | 112.0           |

## 4 Discussion

### 4.1 $T_{\text{stop}}$ and mechanical properties

It is already seen that the NQT tube manufacture process using  $T_{\text{stop}}=600^{\circ}\text{C}$  resulted desired mechanical properties including strength and toughness, while that using  $T_{\text{stop}}=850^{\circ}\text{C}$  failed to achieve properties meeting industrial specifications. The former schedule produced higher volume fraction of non-GB-networked ferrite which enhanced the toughness of the tubes, and produced higher weight fraction of much finer V(C,N) particles which enhanced the strength, so that a desired combination of strength and toughness was obtained. The process using  $T_{\text{stop}}=850^{\circ}\text{C}$  led to not only GB-networked ferrite and coarser precipitates, but also undesired bainite and bainite-like constituents, all of them are extremely harmful to toughness.

These facts also imply that the precipitation characteristics of V in austenite in the schedule using  $T_{\text{stop}}=600^{\circ}\text{C}$  should lead to higher driving force and potential for V(C,N) precipitation and quite different compositions in the austenite phase before phase transformation, compared with in the process using  $T_{\text{stop}}=850^{\circ}\text{C}$ . The large volume fraction of intra-granular ferrite should have a close relation with higher density of fine V(C,N) precipitates in the concerned samples<sup>[10]</sup>.

### 4.2 On the on-line-normalization

In this work, it is found that the austenite did not undergo decomposition during intermediate cooling down to as low as  $600^{\circ}\text{C}$  after tube rolling in the experiment, *i.e.*, no so-called "on-line-normalization" occurred.



In laboratory torsion simulation made by J.J. Jonas and his co-workers<sup>[11]</sup>, it was found that the most effective grain refinement was produced in a medium C-Mn steel and low carbon Ti-V and Nb-V steels when the samples was cooled below the  $A_{r1}$  temperature before entry into the reheat furnace, *i.e.* when an on-line normalization concept was used. However, such a concept is not applicable in present study, unless using a  $T_{\text{stop}}$  as low as 300°C<sup>[4]</sup>.

They also found that the on-line normalization process reduces the precipitation strengthening of the ferrite in microalloyed steels, because it increases the amount of precipitation taking place in the austenite as opposed to the ferrite<sup>[10]</sup>. However, it has been demonstrated in present study that proper selection of the intermediate cooling stop temperature ( $T_{\text{stop}}=600^{\circ}\text{C}$ ) without on-line normalization process would still increase the amount of precipitation in ferrite and the amount of intra-granular ferrite significantly. If a too high  $T_{\text{stop}}$  (say, 850°C) is used, undesired microstructure and mechanical properties will be resulted.

## 5 Main Conclusions

A medium carbon V-Ti-N microalloyed steel designed as a Chinese grade 33Mn2V was used to investigate the evolution of microstructure and precipitates in NQT seamless tube manufacture process, either in laboratory simulation and in industrial scale experiments. This study has led to the following conclusions.

- (1) In the whole thermal and hot rolling process from billets to final tube products, it is found the work-piece should be in austenite state until its decomposition after the stretch-reduction-diameter stage, *i.e.* on-line normalization concept was not used. Thus, the most effective microstructure refinement did not occur in austenite state, but mainly in austenite decomposition following the stretch-reduction-diameter process. It is clear that the intra-granular ferrite formation is very helpful for effective refinement of the whole microstructure.
- (2) About 65% of total precipitates in final tubes were formed in stretch-reduction-diameter and final cooling processes for the schedule with  $T_{\text{stop}}=600^{\circ}\text{C}$ .
- (3) Under such conditions, proper selection of the intermediate cooling stop temperature is of vital

importance in order to achieve desired microstructure and optimized combination of strength and toughness of the finished tubes.  $T_{\text{stop}}=600^{\circ}\text{C}$  has been proved as one suitable choice. Compared with that using a too high  $T_{\text{stop}}$  850°C which may lead to harmful bainite and bainite-like constituents, the NQT tube manufacture schedule using  $T_{\text{stop}}=600^{\circ}\text{C}$  results to finer microstructure and much larger amount of intra-granular ferrite, much larger fraction and finer particle size of precipitates in final tube products.

## References:

- [1] S. Liu, G. Liu, Y. Zhong, et al. Transformation characteristics of medium carbon V-Ti-N microalloyed steel for non-quenched/tempered oil well tubes. *Materials Science and Technology*, 2004(20): 357-362; or refer to its Chinese version: *Iron and Steel*, 2003(38), No.1: 38-42.
- [2] R. Lagneborg, T. Siwecki, S. Zajac, et al. The role of vanadium in microalloyed steels. Swedish Institute for Metals Research, Project Report No: IM-1999-612. August 1999.
- [3] G. Liu, S. Liu, Y. Zhong, et al. Application of vanadium in non-quenched/tempered microalloyed steels used for petroleum casing and tubing. Final Project Report to the Vanadium International Technical Committee and the Chinese Society for Metals, November 2004.
- [4] S. Liu. Study of microstructure evolution in a medium carbon microalloyed steel used for hot-rolling non-quenched/tempered seamless oil-well tubes. Ph.D. Dissertation, University of Science and Technology Beijing, 2004.
- [5] Y. Zhong, G. Liu, S. Liu, et al. Austenite grain growth behavior of steel 33Mn2V designed for oil well tubes. *Acta Metallurgica Sinica*, 2003(39), No.7:699-703 (in Chinese).
- [6] Y. Zhong, G. Liu, S. Liu, et al. Research on dynamic recrystallization law of new steel 33Mn2V for oil well tubes. *Iron and Steel*, 2003(38), No.2: 42-45 (in Chinese).
- [7] F. Wang, G. Liu, Y. Zhang. Thermo-mechanical simulation study on static recrystallization of new steel 33Mn2V for oil well tubes. *Iron and Steel*, 2003(38), No.12: 43-48 (in Chinese).
- [8] F. Wang, G. Liu, Y. Zhang. 3D thermo-mechanical coupled FEM simulation on tube

---

tension-reducing process of 33Mn2V steel for oil well tubes. Journal of University of Science and Technology Beijing, 2004(26), No.5:538-541 (in Chinese).

[9] Y. Yu and G. Liu. Stereology: Principle and application of microstructure quantitative analysis (in Chinese), Beijing: Metallurgical Industry Press, 1989: pages 35- 45.

[10] G. Miyamoto, T. Shinyoshi, J. Yamaguchi, et al. Crystallography of intra-granular ferrite formed on (MnS+V(C,N)) complex precipitate in austenite. Scripta Mater., 2003, 48: 371-377

[11] L.N. Pussegoda, S. Yue, J.J. Jonas. Effect of intermediate cooling on grain refinement and precipitation during rolling of seamless tubes. Materials Science and Technology, 1991, 7: 129-136